QCD in the Early Universe

Michal Šumbera

Nuclear Physics Inst. CAS, 25068 Řež/Prague, Czech Republic and
Faculty of Nuclear Science and Engineering, Czech Technical University, 115 19 Prague, Czech Republic

April 17, 2023

New Trends in Thermal Phases of QCD, Prague, Apr 14-17, 2023

Table of Contents

Introduction

About this Talk

- **Warning:** I am an experimentalist (ALICE@LHC, STAR@RHIC), not a LQCD theorist. Nevertheless, I co-authored several phenomenological papers and review articles utilizing some LQCD results.
- **Disclaimer:** This presentation was initially prepared for an audience with a much lower level of knowledge about the QCD.
- My talk is based in part on the review articles:
  1. A. Addazi, A. Marcianò, T. Lundberg, R. Pasechnik and M. Šumbera, *Cosmology from Strong Interactions*, Universe **8**, no.9, 451 (2022), arXiv:2204.02950.
  2. R. Pasechnik and M. Šumbera, *Different Faces of Confinement*, Universe **7**, no.9, 330 (2021), arXiv:2109.07600.

  and so I will mostly present results published elsewhere by other authors.
- In addition to that I allow myself to speculate, hoping to provoke some discussion.

Matter under Extreme Conditions: Short History

Early Studies

1939 Oppenheimer, Volkoff and Oppenheimer, Snyder studied the gravitational stability of a new phase of neutron matter (gigantic nucleus) suggested by Landau in 1938. Carrying out collapsing matter calculations to $\rho \gtrsim 5 \times \rho_0$ they extrapolated to (black-hole) singularity.

1946 Gamow when discussing the relative abundances of elements in the hot Universe considered a very dense matter with $\rho \approx 1$ eV$\cdot$fm^{-3}.

1962 Zeldovich used the density $\approx 20 \times \rho_0$ to study the limitations of the relativistic EoS of matter made of baryons interacting via a massive vector field.

1965 Penzias and Wilson discovered the CMB radiation providing thus a solid basis for Gamow's hot Universe scenario.

1966 Sakharov established that the absolute maximum of the temperature of any substance in equilibrium with radiation is of the order of Planck temperature $T_P = \sqrt{\frac{\hbar c^5}{G k_B^2}} \approx 10^{19}$ GeV.

Tension Between Bootstrap and Quark Models of Hadrons

1961 Chew and Frautschi published the highly influential article *Principle of Equivalence for All Strongly Interacting Particles . . .* , (aka Bootstrap model of hadrons).

1964 GellMann and Zweig proposed quark model of hadrons.

1965 Hagedorn – Strongly interacting gas of hadrons is a mixture of ideal gases. Each ideal gas component represents one hadron specie. $\Rightarrow$ Heating of the gas leads to the creation of more massive hadron species, but not to the further increase of the gas temperature beyond some limiting, so called Hagedorn temperature ($T_H \approx 170$ MeV).

1969 Bjorken, Bjorken+Paschos and Feynman – Hadron constituents are point-like and move inside the hadrons comparatively freely (Parton model).

1970 Huang and Weinberg: *Current theoretical apparatus is completely inadequate to deal with the thermal history of the Universe.*
Theory does not work even at temperatures $T = 10^{-20} T_P$!!!

Resolution of the Paradox – Asymptotic Freedom

1965 Vanyashin and Terentev found a negative sign in the charge renormalization of charged vector mesons. They attributed this *absurd* result to the non-renormalizability of theory.

1969 Khriplovich correctly calculated the charge renormalization of Yang-Mills theories and found the unusual sign, but a *connection with asymptotic freedom was not made* 't Hooft:1998.

1973 Gross, Wilzek and Politzer (and 't Hooft [unpublished]) discovered the asymptotic freedom in non-Abelian gauge theories.

1975 Collins and Perry – Weakening of the interaction between quarks as they get closer at sufficiently high density leads to de-confinement. The superdense matter at densities higher than the nuclear one consists of a quark soup.

1975 Cabibbo and Parisi: The existence of the limiting temperature T_H signals a second-order phase transition between the hadronic and quark–gluon phases of matter. $\Rightarrow$ First phase diagram of the QCD.

1965 Ivanenko and Kurdgelaidze considered a star made of quarks.

1969 Ivanenko and Kurdgelaidze predicted super-conducting quark phase for the super-dense star interiors.

1970 Itoh mentions the quark matter in the context of neutron stars.

1973 Migdal proposed the phase transition into pion condensate in nuclei and neutron stars.

1974 Lee and Wick suggested to temporarily restore broken symmetries of the physical vacuum by creating abnormal dense states of matter in high-energy collisions of heavy nuclei.

1977 Shuryak introduced the term quark-gluon plasma to describe a new state of matter existing at temperatures above 1 GeV.

1977 Barrois proposed superconducting quark matter.

1983 Bailin and Love predicted the long-range attraction between quarks in $\bar{\mathbf{3}}_c$ channel leading to the color superconductivity with the condensation of ${}^1S_0$ Cooper pairs.

1998 Alford,Rajagopal,Wilczek proposed symmetry breaking pattern $\mathrm{SU(3)_c \times SU(3)_R \times SU(3)_L \times U(1)_B \to SU(3)}_{c+L+R} \times \mathrm{Z(2)}$ leading to the formation of quark Cooper pairs. Breaking of color and flavor symmetries down to the diagonal subgroup $\mathrm{SU(3)}_{c+L+R}$ implies a simultaneous rotation of color and flavor degrees of freedom and is called the color–flavor locking.

2002 Buballa,Hosek,Oertel Color-superconducting two-flavor deconfined quark matter extended to spin-1 Cooper pairing leads to spontaneous breakdown of rotation invariance.

2007 McLerran and Pisarski proposed Quarkyonic Matter situated in between chirally restored and confined matter. It exists at densities parametrically large compared to Λ_{QCD} when the number of colors N_c is large. Because gluons are in adjoint representation of $\mathrm{SU(3)}_c$ their effects are $\sim N_c^2$, and so they dominate all quark-induced $\sim N_c$ effects. $\Rightarrow$ The gluons are permanently confined into glueballs and quarkyonic matter has only N_c d.o.f.

Phase Diagrams of QCD and H_2O

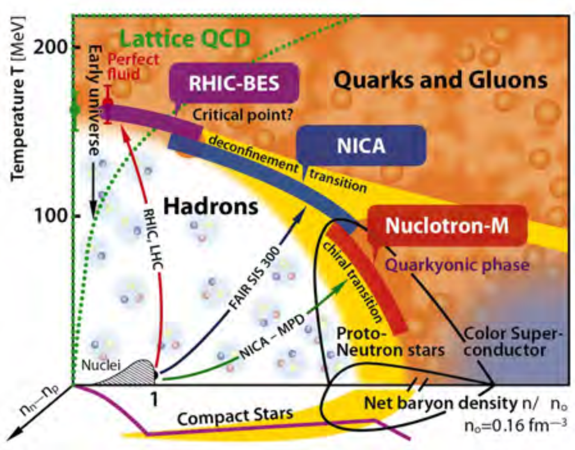

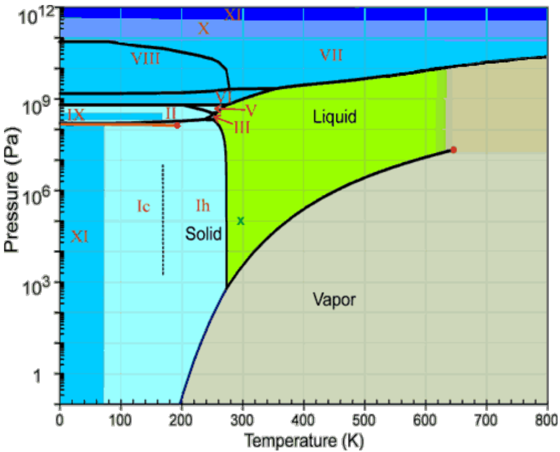

Figure 1: **Left**: QCD phase diagram T vs. (n_B/n_0). [Tejeda-Yeomans:2020].
Right: The phase diagram of water in terms of p and T state variables. The red points mark (p_c, T_c).

High Density Epoch of the Universe

A Brief History of the Universe

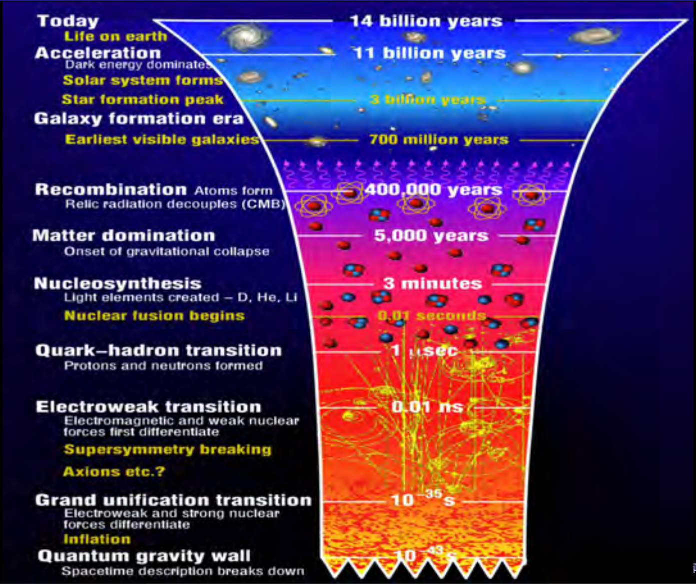

Standard Model Couplings in the Hot Big Bang Era

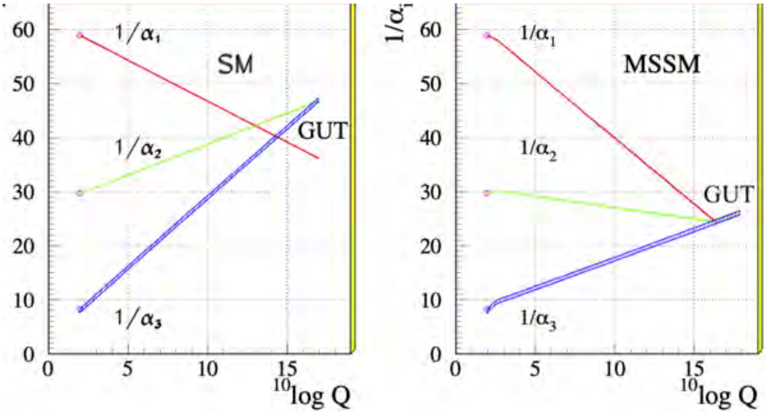

Figure 2: Evolution of the inverse of the three coupling constants $\alpha_1 = \alpha_{\mathrm{EM}}, \alpha_2 = \alpha_{\mathrm{W}}, \alpha_3 = \alpha_{\mathrm{S}}$ in the Standard Model $\mathrm{U(1)_Y \times SU(2)_L \times SU(3)_C}$ (left) and in its supersymmetric extension MSSM (right).

- Change of $\alpha_i(T)$ is very slow (logarithmic).
- Thermodynamics is applicable if the Universe is in global equilibrium.
- Hydrodynamical description needs only local thermal equilibrium (LTE).

The Early Universe in Local Thermal Equilibrium

How do we know that the Early Universe was in the state of LTE? [Mukhanov:2005]

- Collision time among the constituents $t_c = 1/(\sigma n v)$
- LTE $\Leftrightarrow$ Local equilibrium must be reached well before expansion becomes relevant.

$\Rightarrow$ At the cosmic time $t_H \sim 1/H(t)$: $t_c \ll t_H$.

- At $T > T_{\mathrm{EW}}$ all (most of) particles of the SM are ultra-relativistic ($k^2 \gg m^2$) and gauge bosons are massless. $\Rightarrow \sigma \approx \mathcal{O}(1)\alpha^2\lambda^2 \sim \alpha^2/k^2 \sim \alpha^2/E^2 \sim \alpha^2/T^2$,
- For $n \sim T^3, v = 1$ and $\alpha \simeq 10^{-1} - 10^{-2}, \alpha = \alpha_{\mathrm{EM}}, \alpha_{\mathrm{W}}, \alpha_{\mathrm{S}}$:

$$t_c \sim \frac{1}{\alpha^2 T} \ll t_H \sim \frac{1}{H} \sim \frac{1}{\sqrt{\epsilon}} \sim \frac{1}{T^2}.$$

$\Rightarrow$ For $10^{15} - 10^{17}$ GeV $\gtrsim T \gtrsim T_{\mathrm{EW}}$ LTE in expanding fluid persists.

- For $T_{\mathrm{EW}} > T > T_c^{\mathrm{QCD}} \approx 160$ MeV the LTE continues due to large effective cross-section among the particles forming the QGP medium.

What is Changing: Effective Degrees of Freedom

$$g_{\text{eff}}(T) \equiv \frac{\epsilon(T)}{\epsilon_0(T)}\,,\ h_{\text{eff}}(T) \equiv \frac{s(T)}{s_0(T)}\,,\ \epsilon_0(T) = \frac{\pi^2}{30}T^4\,, s_0(T) = \frac{2\pi^2}{45}T^3 \tag{1}$$

$$g^{id}_{\text{eff}}(T) = h^{id}_{\text{eff}}(T) = \frac{7}{8}4N_{\text{F}} + 3N_{\text{V}} + 2N_{\text{V0}} + N_{\text{S}} \tag{2}$$

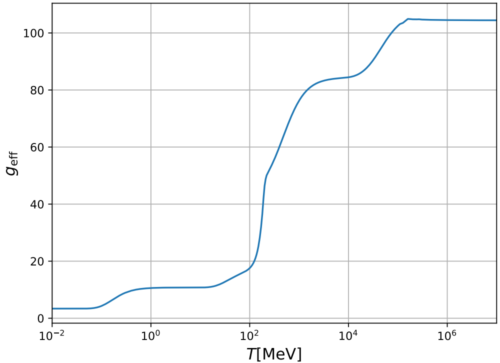

Figure 3: $g_{\text{eff}}(T)$ in the cosmological plasma in the SM, taking into account interactions between particles, obtained with both perturbative and lattice methods. From [Hindmarsh et al. 2020].

Standard Cosmological Model

Einstein equations of general relativity

$$R_{\mu\nu} - \frac{1}{2} g_{\mu\nu}(R - 2\Lambda) = -8\pi G \mathcal{T}_{\mu\nu} \quad (3)$$

$g^{\mu\nu}$ – metric tensor, $R_{\mu\nu} = f(g_{\mu\nu}, \partial_\lambda g_{\mu\nu}, \partial^2_{\lambda,\kappa} g_{\mu\nu})$ – Ricci tensor,
$R = R_{\mu\nu} g^{\mu\nu}$ – scalar curvature, Λ, G – cosmological, gravitational constants,
$\mathcal{T}_{\mu\nu}$ – energy-momentum tensor.

Cosmological principle: the Universe is Homogenous and Isotropic

Solution of (3) preserving space homogeneity and isotropy under its time evolution is spacetime of constant curvature $k = \{+1, 0, -1\}$ with metrics

$$ds^2 = g^{FLRW}_{\mu\nu} dx^\mu dx^\nu = dt^2 - a^2(t)\left[\frac{dr^2}{1 - kr^2} + r^2(d\theta^2 + sin^2\theta d\phi^2)\right] \quad (4)$$

$a(t)$ – scale factor of the Universe connects co-moving (Lagrange) and physical (Euler) coordinates $\hat{r}(t) = a(t)r$.

Early Universe Made Simple

Friedman equation: $g_{\mu\nu}^{FLRW} \rightarrow$ Eq. (3) with $\mu = \nu = 0$

$$H^2(t) \equiv \left(\frac{\dot{a}}{a}\right)^2 = \frac{8\pi G}{3}\epsilon - \frac{k}{a^2} + \frac{\Lambda}{3} \qquad (5)$$

Perfect fluid: $\mathcal{T}_\nu^\mu = diag(\epsilon, -p, -p, -p) \Rightarrow$ Fluid equation

$$\dot{\epsilon} + 3(\epsilon + p)H(t) = 0 \qquad (6)$$

- Ornik,Weiner:1987 Early Universe: $\epsilon \gtrsim 1\text{GeV fm}^{-3} \Rightarrow$ neglect k and Λ in (5) :

$$-\frac{d\epsilon}{3\sqrt{\epsilon}(\epsilon + p)} = \sqrt{\frac{8\pi G}{3}}dt \quad \Rightarrow \quad \dot{\epsilon} + \sqrt{\frac{24\pi G}{3}}(\sqrt{\epsilon}(\epsilon + p(\epsilon)) = 0 \qquad (7)$$

- Integration of (7) using barotropic form of EoS $p(\epsilon)$ yields $\epsilon(t)$.
- **Example:** Time-independent speed of sound $c_s^2 = dp/d\epsilon$ [Sanches et al. 2014]

$$\epsilon(t) = \frac{1}{6\pi G(1 + c_s^2)^2 t^2} \;\Rightarrow\; H(t) \sim \frac{1}{t}, \; \dot{a} \sim t^{-\alpha}, \; \alpha = \frac{1 + 3c_s^2}{3(1 + c_s^2)} \qquad (8)$$

The Bare-bones EoS with the 1st Order Phase Transition

- Simplest EoS incorporating confinement – the MIT bag model [Chodos et al.: 1974]

$$\epsilon_q = \sigma_q T^4 + \mathcal{B},\ p_q = \frac{\sigma_q}{3} T^4 - \mathcal{B} \Rightarrow p_q(\epsilon_q) = \frac{1}{3}(\epsilon_q - 4\mathcal{B}),\ \sigma_q = \frac{\pi^2}{30} g_{\rm eff}^{\rm QCD} \quad (9)$$

$\mathcal{T}^{\mu\mu}(T) = \Delta\epsilon = \epsilon_q(T_c) - \epsilon_h(T_c) = 4\mathcal{B},\ T_c \approx 0.67\mathcal{B}^{1/4} \approx 150$ MeV.

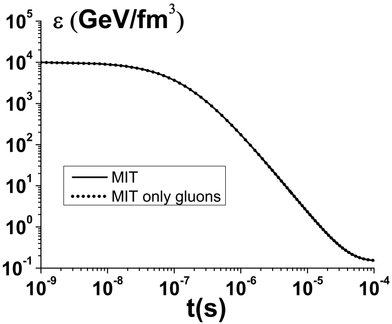

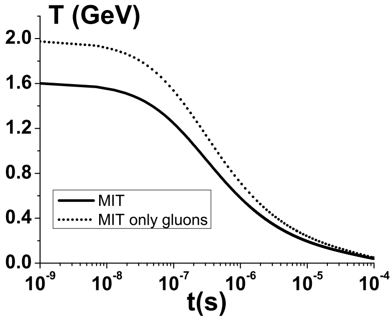

Figure 4: Solution of Eq. (7) using the MIT BM EoS (9) with $\epsilon_0(t_0) = 10^4$ GeVfm^{-3} and $t_0 = 10^{-9}$s. **Left**: $\epsilon(t)$. [Sanches et al.:2014] **Right**: $T(t)$.

Modified Bag Model EoS

$$\epsilon(T) = \sigma T^4 - CT^2 + \mathcal{B}\,, \qquad p(T) = \frac{\sigma}{3} T^4 - DT^2 - \mathcal{B}\,. \tag{10}$$

- $C = D > 0$: LQCD motivated "fuzzy" bag model EoS [Pisarski:2006, Megias:2007].
- $C = -D < 0$: Gluonic q-particle EoS with $\mathcal{B}(T) = -CT^2 + \mathcal{B}$ [Schneider:2001].
- The barotropic form of the EoS is obtained from

$$T^2(\epsilon) \equiv \frac{C + \sqrt{C^2 + 4\sigma(\epsilon - \mathcal{B})}}{2\sigma} > 0 \tag{11}$$

$$p(\epsilon) = \frac{1}{3}(\epsilon - 4\mathcal{B}) - \frac{1}{3} sgn(A)|A|T^2(\epsilon),\ \ A = 3D - C\,. \tag{12}$$

$$c_s^2(\epsilon) = \frac{dp(\epsilon)}{d\epsilon} = \frac{1}{3}\left(1 - \frac{sgn(A)|A|}{\sqrt{C^2 + 4\sigma(\epsilon - \mathcal{B})}}\right) \geq 0\,. \tag{13}$$

- For $A > 0$ there is a lower bound on energy density: $\epsilon > \epsilon_0 = \frac{A^2 - C^2}{4\sigma} + \mathcal{B}\,.$ (14)
- For $A < 0$ $p(\epsilon)$ has two independent components and peak in $\Theta \equiv \frac{\mathcal{T}^{\mu\mu}(T)}{T^4} = \frac{\epsilon_q - 3p_q}{T^4}$.

Equation of State Based on the Fundamental Theory

- In the SM $$p_B(T) = \lim_{V\to\infty} \frac{T}{V} \ln \mathcal{Z}(T,V)$$

$$\mathcal{Z}(T,V) = \exp\left[\frac{p_B(T)V}{T}\right], \; p_B(T) = p_E(T) + p_M(T) + p_G(T) \tag{15}$$

- p_B is the "bare" result related to the physical (renormalized) pressure as $p(T) = p_B(T) - p_B(0)$.
- $p_E(T), p_M(T), p_G(T)$ collect the contributions from the momentum scales $k \sim \pi T$, $k \sim gT$, and $k \sim g^2 T/\pi$, respectively.
- Couplings of SM are $g \in \{h_t, g_1, g_2, g_3\}$, where h_t is the Yukawa coupling between the top quark and the Higgs boson, and g_1, g_2, g_3 are related to $U_Y(1)$, $\mathrm{SU_L}(2)$ and $\mathrm{SU}_c(3)$ gauge groups, respectively.
- Calculations of the dimensionless function $p(T)/T^4$ and of the trace anomaly $\Theta(T)$ up to $\mathcal{O}(g^5)$ were performed in [Laine,Mayer:2015].

The EoS from the SM and GUT

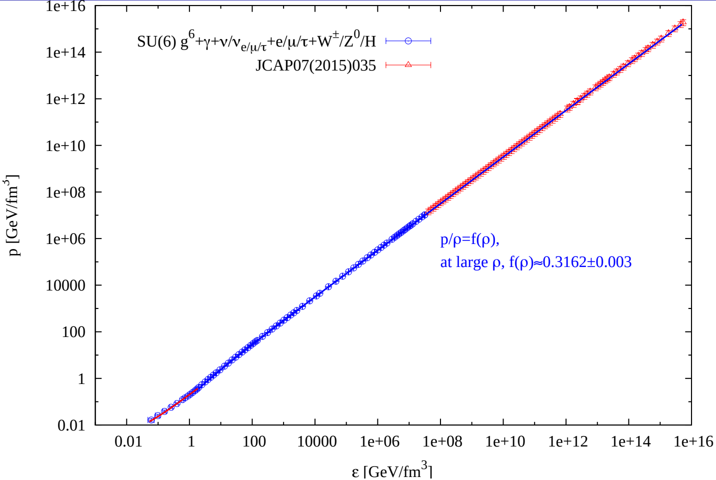

Figure 5: Combined EoS $p(\epsilon), \epsilon \equiv \rho$ of QCD and EW matter, using lattice results of [Borsanyi et al:2016] extended to include other DoFs such as γ, neutrinos, leptons, EW, and Higgs bosons as well as perturbative results of [Laine,Mayer:2015]. Adapted from [Tawfik,Mishustin:2019].

The EoS parametrization

- GUT EoS (△ in Fig. 5) $p_{\rm GUT} = (0.330 \pm 0.024)\epsilon$ valid for $10^8 \lesssim \epsilon \leq 10^{16}$ GeV·fm^{-3} is already in the ideal gas limit.
- Hadronic-era EoS $p_h = (0.003 \pm 0.002) + (0.199 \pm 0.002)\epsilon$ is used for $\epsilon \lesssim 1$ GeV·fm^{-3}.
- Combined EoS for QCD and EW eras has two independent contributions $p_1(\epsilon)$ and $p_2(\epsilon)$.

$$p_{\rm SM} = p_1(\epsilon) + p_2(\epsilon)\,, \quad p_1(\epsilon) = b\epsilon\,, \quad p_2(\epsilon) = a + c\epsilon^d \tag{16}$$

$$a = 0.048 \pm 0.016,\ b = 0.316 \pm 0.031,\ c = -0.21 \pm 0.014,\ d = -0.576 \pm 0.034$$

- Critical density ϵ_c defined implicitly $p_h(\epsilon_c) = p_{\rm SM}(\epsilon_c)$ reads: $\epsilon_c \simeq (1.2 \pm 0.2)$ GeV·fm^{-3}.
- While $p_1(\epsilon) > 0\ \forall\epsilon$, the second component has $p_2 < 0$ up to $\epsilon \lesssim (7 - 13)$ GeV·fm^{-3}.

Interpreting the QCD+ EW Era Parametrization

- $p_1(\epsilon) \approx \frac{1}{3}\epsilon$ (ideal gas of massles particles EoS).
- $p_2(\epsilon) = -\mathcal{B}(\epsilon) = a + c\epsilon^d$ – density-dependent bag function, cf. Eq. (9) (instanton liquid?)
- The sound velocities of both components are positive:

$$c_{s,1}^2(\epsilon) = \frac{dp_1}{d\epsilon} = b > 0\,, \qquad c_{s,2}^2(\epsilon) = \frac{dp_2}{d\epsilon} = c \cdot d \cdot \epsilon^{d-1} > 0 \tag{17}$$

$\Rightarrow$ May the second component correspond to real matter?

- $a \approx 0 \Rightarrow$ EoS $p_2(\epsilon) \approx c\epsilon^d, c < 0, d < 0$ coincides with generalized Chaplygin EoS* which was applied to cosmological scenarios as a plausible model for DE [Kamenshchik et al:2001].

---

*) The EoS $p = -A/\rho$ has its origin in the study of lifting forces on an airplane's wing. [Chaplygin 1904], [von Kármán 1941]

Strongly Coupled and Saturated Regimes of QCD

Evolution of the Strong Coupling Constant $\alpha_s(Q)$

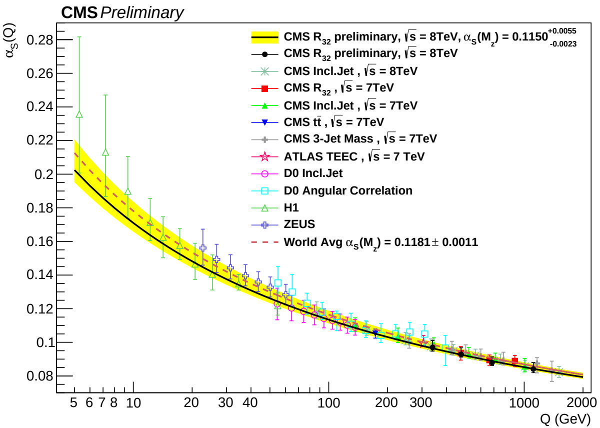

Figure 6: $\alpha_S(Q)$ obtained from MSTW2008 NLO PDF set. [CMS:2017].

- For $0.2 \lesssim \alpha_S \lesssim 0.08$ "temperatures" $T \approx Q/(2\pi) \in (1, 200)$ GeV are reachable?.

The Plasma of Charged Particles

- Plasma $=$ system of mobile charged particles [Ichimaru:1982].
- Electrically neutral gas (liquid, crystal) at high temperatures T turns into a system of charged particles with the long-range $U(1)$ interaction.
- Plasma interaction parameter

$$\Gamma_{\rm EM} = \frac{q^2}{r_s k_B T} \sim \frac{U_{int}}{E_{th}}, \qquad r_s = \left(\frac{3V}{4\pi N}\right)^{1/3} \approx 0.62 n^{-1/3}, \tag{18}$$

  q - particle charge

  r_s - average inter-particle distance (Wigner-Seitz radius)
- Strongly-coupled (SC) plasma: $\Gamma_{\rm EM} > 1$, i.e. when $U_{int} > E_{th} \sim k_B T$, interaction energy prevails over thermal energy of the plasma particles.
- **Example** Table salt – crystalline plasma made of permanently charged Na^+ and $C\ell^-$ ions. $\Gamma_{\rm EM} \approx 60$ at $T \approx 10^3$K. [Shuryak:2008].

QCD Plasma: The Phenomenologic Approach

The Plasma of Quarks and Gluons

- Generalization $U(1) \to SU(3)_c$ [Thoma:2005], see also [Bannur:2005]

$$\Gamma_{\rm QCD} \simeq 2\frac{C_{q,g}\alpha_{\rm S}}{r_s T}\,, \quad C_q = \frac{N_c^2-1}{2N_c} = \frac{4}{3}\,, \quad C_g = N_c = 3 \tag{19}$$

N.B. In relativity chromo-electric $\approx$ chromo-magnetic $\Rightarrow$ 2 in (19).

- For ideal massless QCD gas with N_F active quarks and $d_F = g_{\rm eff}^{\rm QCD}$

$$n = d_F \frac{\zeta(3)}{\pi^2} T^3 \approx d_F \left(\frac{T}{2}\right)^3, d_F = 2\times 8 + \tfrac{7}{8}(3\times N_F \times 2\times 2) \tag{20}$$

$$r_s \simeq 1.24 d_F^{-1/3} T^{-1} \Rightarrow r_s T = f(N_F(T)) \tag{21}$$

1. $T \approx 200$ MeV: $\alpha_{\rm S} = 0.3-0.5$, $N_F = 2$, $d_F = 37 \Rightarrow \Gamma_{\rm QCD} \simeq 2-8$.
2. $T \simeq T_{\rm EW}$: $\alpha_{\rm S} = 0.08$, $N_F = 5$, $d_F = 52.5$ and $\Gamma_{\rm QCD} \simeq 0.5-1.5$.
3. $T \gg T_{\rm EW}$: $N_F = 6$, $\Gamma_{\rm QCD}(T)$ is solely driven by $\alpha_{\rm S}(T) \sim -\ln T$.

The Weakly Interacting QCD: DGLAP and BFKL

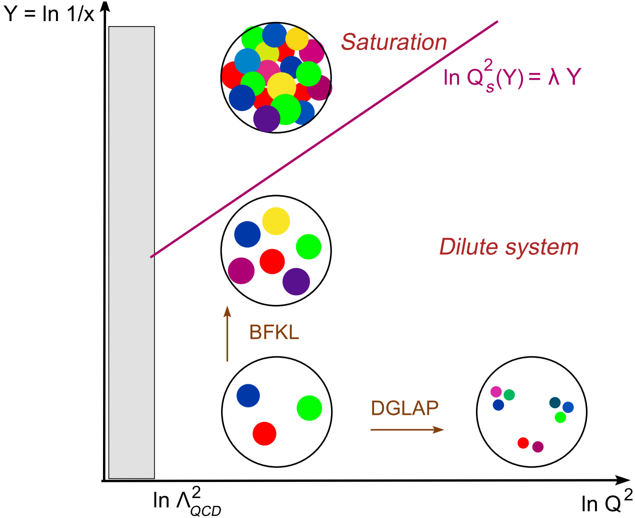

Figure 7: Parton density and size as a function $Y = \ln(1/x)$ and $\ln Q^2$. From [Gelis et al:2010].

QCD at High Parton Densities and Saturation

[Gribov jr.,Levin,Ryskin:1983] , [McLerran,Venugopalan:1993]

- Partons "overlap" when $\sigma_{gg} \sim \alpha_S/Q^2$ times $xG_A(x,Q^2)$ – the probability to find at fixed Q a parton carrying a fraction x of the parent parton momentum – becomes comparable to the geometrical cross section πR_A^2 of the object A occupied by the gluons.

$$Q_s^2(x) = \frac{\alpha_S(Q_s)}{2(N_c^2-1)} \frac{xG_A(x,Q_s^2)}{\pi R_A^2} \sim \frac{1}{x^\lambda} \Rightarrow \ \ln Q_s^2(x) = \lambda Y \qquad (22)$$

- $Q_s(x)$ – Fixed point of the PDF evolution in x or, equivalently, the emergent "close packing" scale
- Repulsive gg interactions $\Rightarrow$ occupation number f_g (# of gluons with a given x times the area each gluon fills up divided by the transverse size of the object) saturates at $f_g \sim 1/\alpha_S$.
- The same scaling as for the Higgs condensate, superconductivity or the inflaton field in the very early Universe.

The Glasma as a (Semi-)Classical Matter

QCD in the classical regime [Kharzeev:2002]

- Introduce coupling-independent field tensors

$$A_\mu^a \to \mathcal{A}_\mu^a \equiv g_\mathrm{S} A_\mu^a, \quad g_\mathrm{S}^2 = 4\pi\alpha_\mathrm{S}$$

$$F_{\mu\nu}^a \to g_\mathrm{S} F_{\mu\nu}^a \equiv \mathcal{F}_{\mu\nu}^a = \partial_\mu \mathcal{A}_\nu^a - \partial_\nu \mathcal{A}_\mu^a + f^{abc} \mathcal{A}_\mu^b \mathcal{A}_\nu^c \,, \tag{23}$$

- Calculate action of the gluon field

$$S_g = -\frac{1}{4} \int F_{\mu\nu}^a F^{\mu\nu,a} d^4x = -\frac{1}{4g_\mathrm{S}^2} \int \mathcal{F}^{\mu\nu,a} \mathcal{F}_{\mu\nu}^a d^4x \tag{24}$$

- Gluon occupation number $$f_g \sim \frac{S_g}{\hbar} = \frac{1}{\hbar g_\mathrm{S}^2} \rho_4 V_4 \tag{25}$$

  where $\rho_4 \sim \langle \mathcal{F}^{\mu\nu,a} \mathcal{F}_{\mu\nu}^a \rangle$ is four-dimensional gluon condensate density.

- Saturated gluon matter is weakly coupled.
- The limits $g_\mathrm{S}^2 \to 0$ and $\hbar \to 0$ are equivalent! $\Rightarrow$ weakly interacting means semi-classical.

The CGC–Black Hole correspondence

- Dvali,Venugopalan:2021 Correspondence between Black Holes as highly occupied condensates of N weakly interacting gravitons and CGCs as highly occupied gluon states.
- Both BH and CGC attain a maximal entropy S_{max} permitted by unitarity when the occupation number f and the coupling α of the respective constituents (gravitons, gluons) satisfy $f = 1/\alpha(Q_s)$, where Q_s represents the point of optimal balance between the kinetic energies of the individual constituents and their potential energies.
- S_{max} equals the area in units of the Goldstone constant corresponding to the spontaneous breaking of Poincare symmetry[1] by the corresponding graviton or gluon condensate.
- In gravity, the Goldstone constant is the Planck scale, and gives rise to the Bekenstein-Hawking entropy.
- In the CGC, the Goldstone scale is determined by the onset of gluon screening.

[1] see e.g. [Low,Manohar:2002]

Early Universe Filled with the Glasma?

- Consider partons in the Universe at fixed temperature $T \cong Q/2\pi$.
- $Q_s^2(x) \sim \alpha_S(T) \sim 1/\ln(T)$, $a(t) \sim t^{1/2}$.
- For ideal massless gas EoS $\epsilon \sim T^4 \sim a^{-4}$, and hence $T \sim a^{-1} \sim R_A^{-1}$. $\Rightarrow$ $Q_s^2(x) \sim \alpha_S(T) R_A(T) \sim 1/(T \ln T)$
- McLerran,Venugopalan:1993: *distribution functions for quarks and gluons are computable at small x for sufficiently large nuclei, perhaps larger than can be physically realized.*
- Early Universe = very big nucleus with $R_A \ggg 1$ fm filled with the gluons $\Rightarrow$ the saturation limit is easily reachable even with $x \simeq 1$ gluons.
- At $T \approx T_{EW}$ for YM bosons $g_{\rm eff}^{\rm QCD}/g_{\rm eff}^{\rm EW} \simeq 8/3 \Rightarrow$ Glasma might have been prevalent form of matter also during EW era.
- $T \gg T_{EW}$: the gluon exchange between quarks (antiquarks) becomes surpassed by the exchange of EW massless gauge bosons $W^{\pm}, W^0, B^0, \ldots$ ...GUT YM bosons can also form the classical condensate.

Glass properties of the Glasma and Early Universe

- In condensed matter physics glass is a non-equilibrium, disordered state of matter acting like solids on short time scales but liquids on long time scales [Sethna:2021].
- Two scales of glasma: $$\tau_{\rm wee} = \frac{1}{k^-} = \frac{2k^+}{k_\perp^2} = \frac{2xP^+}{k_\perp^2} \ll \frac{2P^+}{k_\perp^2} \approx \tau_{\rm valence} \,. \qquad (26)$$
  $\Rightarrow$ Valence modes are static over the time scales of wee modes [Berges:2020].
- Glasses are formed when liquids are cooled too fast to form the crystalline equilibrium state. This leads to an enormous # of possible configurations $N_{\rm gl}(T)$ into which the glasses can freeze $\Rightarrow$ large entropy $S = \ln N_{\rm gl}(T)$, such that $S(T=0) > 0$, [Sethna:1988].
- For CGC fast cooling occurs during the GUT era ($\sim 1/3$ of gauge bosons are gluons). By the end of that period, the excess of effective entropy DoF $h_{\rm eff}$ is almost completely absorbed by the saturated gluonic matter.
- The gluon condensation leads to the formation of many glasma domains with completely different gluonic configurations $\Rightarrow$ CGC matter in Early Universe had $h_{\rm eff}^{\rm QCD} \gg g_{\rm eff}^{\rm QCD}$.

Creation of Primordial Black Holes During the Phase Transitions

Beyond the SCM: Metrics Fluctuations

- Inhomogeneities of matter filling the early Universe are described by the metric perturbations $\delta g_{\mu\nu}$.
- They can be decomposed into three irreducible pieces – scalar, vector and tensor ones.
- The scalar part is induced by energy density fluctuations $\delta\epsilon$, the vector and tensor perturbations are related to the rotational motion of the fluid and to the gravitational waves, respectively.

Scalar metrics fluctuations

- Can lead to the matter collapsing into primordial black holes (PBHs).
- Proposed half-century ago by Zeldovich and Novikov: 1967 and by Hawking: 1971.
- Carr and Hawking constrained the spectral index of the primordial fluctuation spectrum.
- Niemier and Jedamzik: 1997 used scaling and self-similarity arguments to predict formation of microscopic PBHs at all epochs.

Evolution of the Early Universe

Cooling of the Universe: The Insight from the Asymptotic Freedom

The Universe cooled down via series of first- or second-order phase transitions (PTs) associated with the various spontaneous symmetry breakings (SSBs) of the basic non-Abelian gauge fields, see e.g. the classical textbooks [Linde:1978], [Bailin and Love:2004], [Boyanovsky et al:2006].

Standard Model Predicts Two Phase Transitions

1. At $T \sim m_H$ the PT responsible for the SSB of the electroweak (EW) symmetry occurs. It provides masses to elementary particles.
   The lattices calculations show that for $m_H \geq 67$ GeV this PT is an analytic crossover [Kajantie et al.:1996], [Csikor et al.:1999].

2. At $T < 200$ MeV the SSB of the chiral symmetry of the $SU(3)_c$ color group, the QCD, takes place. Its nature affects the evolution of the Early Universe. In a strong first-order PT scenario, the de-confined matter supercools before bubbles of hadron gas are formed. $\Rightarrow$ The inhomogeneities in this phase could have a strong effect on the nucleosynthesis epoch.

Reminder: Effective Degrees of Freedom

$$g_{\text{eff}}(T) \equiv \frac{\epsilon(T)}{\epsilon_0(T)}\,,\;\; h_{\text{eff}}(T) \equiv \frac{s(T)}{s_0(T)}\,,\;\; \epsilon_0(T) = \frac{\pi^2}{30}T^4\,, s_0(T) = \frac{2\pi^2}{45}T^3 \tag{27}$$

$$g^{id}_{\text{eff}}(T) = h^{id}_{\text{eff}}(T) = \frac{7}{8}4N_{\text{F}} + 3N_{\text{V}} + 2N_{\text{V0}} + N_{\text{S}} \tag{28}$$

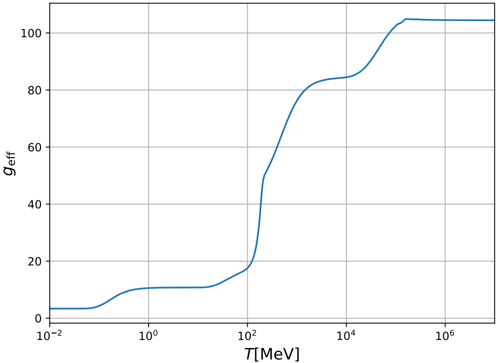

Figure 8: $g_{\text{eff}}(T)$ in the cosmological plasma in the SM, taking into account interactions between particles, obtained with both perturbative and lattice methods. From Hindmarsh et al.:2020.

Cosmological Parametrization of the EoS

- In cosmology the EoS is parametrized as $p = w\epsilon$

$$w(T) = \frac{sT}{\epsilon} - 1 = \frac{4h_{\rm eff}(T)}{3g_{\rm eff}(T)} - 1 \tag{29}$$

$$c_s^2(T) = \frac{dp}{d\epsilon} = T\frac{ds}{d\epsilon} + s\frac{dT}{d\epsilon} - 1 = \frac{4}{3}\left[\frac{4h_{\rm eff}(T) + Th'_{\rm eff}(T)}{4g_{\rm eff}(T) + Tg'_{\rm eff}(T)}\right] - 1 \tag{30}$$

where the prime indicates differentiation with respect to T.

- Causality: $$c_s \leq 1 \quad \Rightarrow \quad \frac{h_{\rm eff}(T)}{g_{\rm eff}(T)} \leq \frac{3}{2}\,, \tag{31}$$

upper bound at $w = 1$ corresponds to absolutely stiff fluid [Zeldovich:1961].

- N.B. $w = \bar{w} = const.$ corresponds to $h_{\rm eff}(T)/g_{\rm eff}(T) = const(T)$.

Creation of Primordial Black Holes During Phase Transitions

- PBHs form more easily during cosmic phase transitions and annihilation epochs than during a pure radiation-dominated phase.
- The softest point (SP) – a local minimum in $w = p/\epsilon$ (and hence also in c_s) – leads to elongation of the expansion time of the matter.
- Consider cooling period $T_1 < T < T_2$, $w(T) < w(T_{1,2}) = \frac{1}{3}$ around the local minimum $w(T_{\rm SP})$, $T_1 < T_{SP} < T_2$ and define [Carr et al.:2019]

$$\Delta h_{\rm eff}(T) \equiv g_{\rm eff}(T) - h_{\rm eff}(T), \; \Delta h_{\rm eff}(T_2) = \Delta h_{\rm eff}(T_1) = 0 \quad (32)$$

- For $w(T) < 1/3; \;\; \Delta h_{\rm eff}(T) > 0$, cf. eq. (30).
  $\Rightarrow$ Initial drop in $h_{\rm eff}(T)$ always precedes the jump in $g_{\rm eff}(T)$.
  $\Rightarrow$ Concentrate on T when part of the radiation transforms into NR matter.

QCD: Long-lived fireball as a signature of QGP to hadron phase transition [Hung,Shuryak:1994].

LQCD: Local minimum $w = 0.145(4)$ at $T = 159(5)$ MeV [Borsanyi et al:2010].

NR Particles and the EoS of the Early Universe

1. For EW PT drop in $g_{\rm eff} = 106.75 \to 86.75$ happens nearly at the same time at $T \sim m_{\rm t} \sim m_H \sim m_Z \sim m_W$.
2. After that (neglecting changes at the b,c-quark and τ-lepton thresholds) $g_{\rm eff}$ remains constant down to QCD PT at $T \approx 160$ MeV when $g_{\rm eff} \to 17.25$
3. Pions and muons become NR, yielding $g_{\rm eff} = 10.75$.
4. $g_{\rm eff}$ remains constant until e^+e^- annihilation and neutrino decoupling at $T \approx 1$ MeV, when it drops down to $g_{\rm eff} = 3.36$.

- In each of these transformations first $h_{\rm eff}(T) \downarrow$ at $T_2 > T > T_{\rm SP}$ followed later on by $g_{\rm eff}(T) \downarrow$ at $T_{\rm SP} < T < T_1$.
- Abrupt reduction of $g_{\rm eff}(T)$ leads to a sudden drop in $c_s(T)$, cf. eq. (30), and hence to a drop of $p = w(T)\epsilon$, cf. eq. (29).
- Entropy lost by the radiation during its cooling $\sim \Delta h_{\rm eff}(T_{\rm SP})$ is dumped into the collapsing matter forming the PBH.

"Coarse-grained" Scenario for the PBH Formation

- LIGO/Virgo may probe QCD PT and lepton flavour asymmetries associated with a pion condensation phase [Carr et al.:2019].
- Far more entropy in supermassive black holes in galactic centers than in all other sources of entropy put together [Penrose:2018].

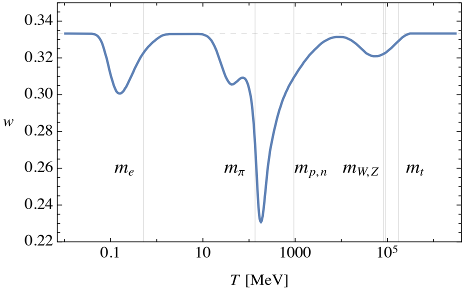

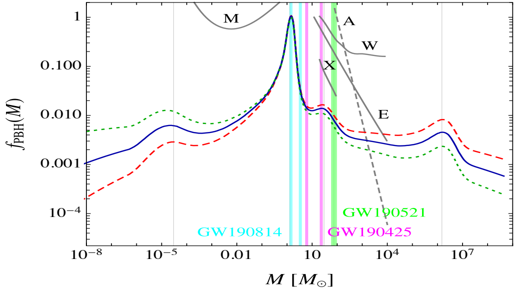

Figure 9: **Left:** $w(T)$. Vertical lines correspond to the EW and QCD PTs and e^+e^- annihilation. **Right:** The mass spectrum of PBHs $f_{\rm PBH}(M)$ in Solar mass units $M_\odot$. Vertical coloured lines indicate the masses of the three LIGO-Virgo events. Grey curves are constraints from different observations. [Carr et al.:2019]

PBH Formation During the QCD Phase Transition Musco et al.:2023

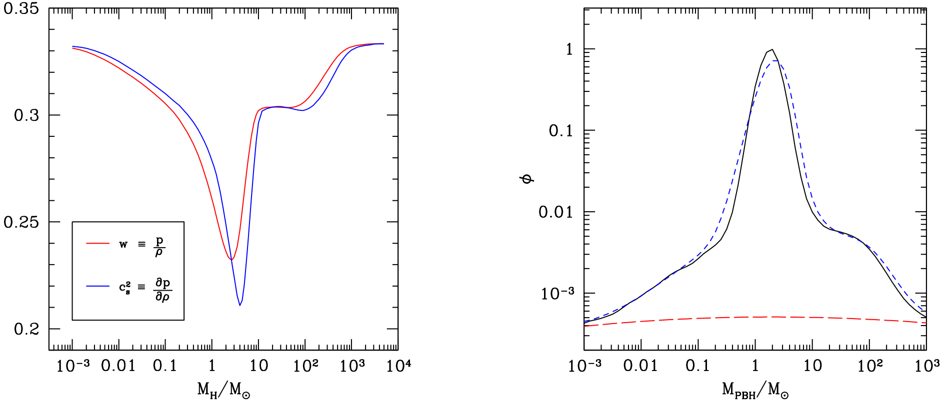

- $R_H d\Phi/dR_H + (5+3w)/[3(1+w)]\Phi = 1$, for $p/\rho = \bar{w} = const.$ $\bar{\Phi} = 3(1+\bar{w})/(5+3\bar{w})$
- Even though the reduction of c_s and w is quite small $\sim 10\%$, for scale-invariant, Gaussian primordial curvature fluctuations of cosmologically interesting amplitude, PBH formation is a factor $\sim$1000 more likely during the QCD epoch than before or after.

Summary

Take-Homme Message

- QCD represents a fruitful theory when applied to the early history of our Universe.
- Although the LQCD and LQCD-motivated models play an important role in establishing the correct EoS of the Early Universe one must be careful when translating its results into a viable phenomenology.
- Saturated and strongly interacting QCD matter might have played an important role in the evolution of our Universe over a broad range of temperatures $T_P \gtrsim T \gtrsim T_{QGP}$.
- QGP to hadron phase transition very likely leaves its imprint primordial black holes with masses $5M_\odot \gtrsim M_{\mathrm{P}BH} \gtrsim M_\odot$.

Thank you for your attention!